An Experimental and Theoretical Investigation of the Olefinic Carbon Chemical Shift Tensors in *trans*-Stilbene and Pt(η^2-*trans*-stilbene)(PPh_3)$_2$

Guy M. Bernard, Gang Wu,† and Roderick E. Wasylishen*

Department of Chemistry, Dalhousie University, Halifax, Nova Scotia, Canada B3H 4J3

Received: December 17, 1997; In Final Form: February 16, 1998

The olefinic carbon chemical shift tensors of *trans*-stilbene-α,β-$^{13}C_2$ (**1**) and (*trans*-stilbene-α,β-$^{13}C_2$)[bis-(triphenylphosphine)]platinum(0) (**2**) have been characterized by solid-state ^{13}C NMR spectroscopy. Analyses of the ^{13}C NMR spectra obtained for stationary powder samples of **1** and **2** at 4.7 and 9.4 T yield the principal components of the carbon chemical shift tensors. The presence of a homonuclear spin pair in these compounds provides information about the orientation of the chemical shift tensors in the dipolar frame of reference. The span, Ω, and skew, κ, of the olefinic carbon chemical shift tensor of **1** are 166 ppm and −0.145, respectively, comparable to those of other known olefinic carbons. The carbon chemical shift is largest when the applied magnetic field is in the plane of the vinyl group, perpendicular to the olefinic C,C bond (δ_{11} = 215 ppm) and smallest when it is perpendicular to the vinyl group (δ_{33} = 49 ppm). The intermediate principal component of the chemical shift tensor, δ_{22} = 120 ppm, is oriented along the olefinic C,C bond. Upon coordination to platinum(0), the isotropic carbon chemical shift changes from 128 to 68 ppm, and the span of the chemical shift tensor decreases dramatically, Ω = 51 ppm. The experimental results are compared with those from ab initio shielding calculations performed with a combination of density functional theory (DFT) and the gauge-including atomic orbitals (GIAO) method. Overall, agreement with experiment is good. The combined experimental and theoretical approach allows one to suggest the most likely orientation of the carbon chemical shift tensor for **2** in the molecular axis system.

Introduction

Transition-metal olefin complexes are important organometallic compounds, since they are essential intermediates in a wide variety of homogeneous catalytic processes.[1] In platinum(II)−olefin complexes, which are typical model compounds for square-planar complexes, the olefinic C,C bond is usually slightly longer than that of the free ligand and is oriented approximately perpendicular to the plane containing the remaining ligands. In contrast, for Pt(0)−olefin complexes, typical trigonal-planar compounds, the olefinic C,C bond lies in the plane containing the other ligands (Figure 1) and is lengthened significantly compared to its value in the free ligand.[1]

The isotropic carbon chemical shift (CS) of olefinic carbons has been used extensively over the past 20 years for the study of metal−olefin complexes in solution.[2,3] For example, upon coordination with Pt(0), the nuclear magnetic shielding increases 60−80 ppm compared to the corresponding free ligand value.[4] However, there have been few solid-state ^{13}C NMR studies dealing with chemical shift *tensors* of the olefinic carbons in metal−olefin complexes. Wallruff[5] studied solid-state ^{13}C NMR spectra of a series of metal−diene complexes and obtained the principal components of their olefinic carbon CS tensors. In a recent study, Huang et al.[6] reported the principal components of the olefinic carbon CS tensor in Zeise's salt and Zeise's dimer; the orientation of the carbon CS tensor for the former compound has been reported elsewhere.[7] Gay and Young also reported the principal components of carbon CS tensors for several metal−olefin complexes.[8] However, apart from Zeise's salt, only the magnitudes of the principal components of the olefinic carbon CS tensors have been reported. To our knowledge, no other olefinic carbon CS tensor orientations in transition-metal complexes have been reported, although it is noted that Wang and Ellis[9] characterized the carbon CS tensor of ethene adsorbed on a Ag/γ-alumina surface.

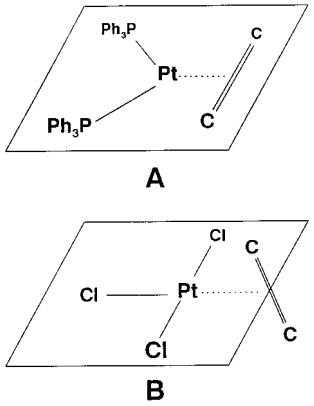

Figure 1. A typical Pt(0)−olefin complex (A), showing the planar orientation of the olefin with respect to the platinum and the other subsitutents, and a typical Pt(II)−olefin complex (B), with the olefin oriented perpendicular to the plane containing the platinum and its substituents.

Here we report solid-state ^{13}C NMR determinations of the olefinic carbon CS tensors in *trans*-stilbene-α,β-$^{13}C_2$ (**1**) and its zerovalent platinum complex, (η^2-*trans*-stilbene-α,β-$^{13}C_2$)-[bis(triphenylphosphine)]platinum(0) (**2**) (Scheme 1). By introducing double ^{13}C-labeling in the olefinic carbons of the

† Present address: Department of Chemistry, Queen's University, Kingston, Ontario, Canada K7L 3N6.

* To whom all correspondence may be addressed. Phone (902)494-2564; Fax (902)494-1310; E-mail RODW@IS.DAL.CA.

S1089-5639(98)00558-1 CCC: $15.00
Published on Web 04/11/1998

SCHEME 1: Molecular Structures of *trans*-Stilbene, 1, Pt(*trans*-stilbene)(PPh_3)$_2$, 2, Pt(*trans*-stilbene)(PMe_3)$_2$, 3, and Pt(ethene)(PMe_3)$_2$, 4

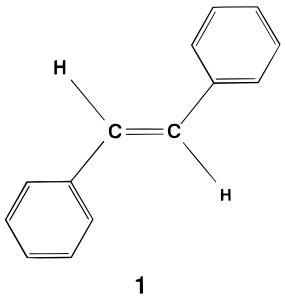

1

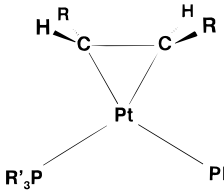

2: R = R' = Ph.

3: R = Ph; R' = Me.

4: R = H; R' = Me.

trans-stilbene ligand and by analyzing the ^{13}C NMR spectra of stationary powder samples, we were able to (1) obtain the magnitudes of the principal components of the olefinic carbon CS tensors and (2) determine their orientations relative to the ^{13}C,^{13}C dipolar vector. The CS tensor orientations relative to the molecular frame were determined by comparing the experimental results with those calculated using DFT in combination with the gauge-including atomic orbitals (GIAO)[10] method.

Theoretical Background

1. Solid-State NMR Spectra of Dilute Spin $^1/_2$ Nuclei. The characterization of the symmetric portion of a CS tensor entails the determination of six parameters: the three principal components of the CS tensor and the three Euler angles defining their orientation in the molecular framework (Figure 2).[11] These parameters may be determined from single-crystal NMR experiments in which the chemical shift is observed as a function of the crystal orientation in the magnetic field, but such experiments are often time-consuming, and single crystals of sufficient size and quality are not always available. If powder samples are investigated, the principal components of the CS tensor may be determined; however, information concerning the orientation of the CS tensor is generally not available. The chemical shielding at a nucleus varies with the orientation of the molecule in the applied magnetic field; thus, the NMR resonance frequency is orientation-dependent:

$$\nu_i = \nu_0[1 - (\sigma_{11}\sin^2\theta\cos^2\phi + \sigma_{22}\sin^2\theta\sin^2\phi + \sigma_{33}\cos^2\theta)] \quad (1)$$

In eq 1, ν_0 is the Larmor frequency and the angles θ and ϕ orient the magnetic field in the principal axis systm (PAS) of the CS tensor, as shown in Figure 3. The σ_{ii} denote the principal components of the chemical *shielding* tensor relative to the bare nucleus, with $\sigma_{33} \geq \sigma_{22} \geq \sigma_{11}$. Experimentally, one measures a chemical *shift* tensor relative to a given reference. These are denoted from least to most shielded such that $\delta_{11} \geq \delta_{22} \geq \delta_{33}$. Thus, for example, δ_{11} corresponds to σ_{11} and is the highest-frequency component. In the case of ^{13}C NMR, the principal components of the chemical shift tensor are measured relative to the isotropic chemical shift of TMS.

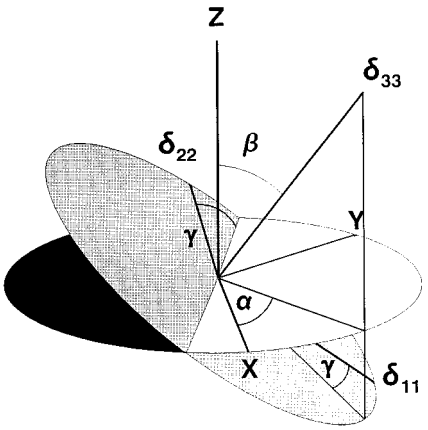

Figure 2. Orientation of the chemical shift tensor with respect to the molecular framework. The transformation from one axis system to another is achieved by rotating by an angle α about *Z*, rotating by an angle β about the new *Y*, the intersection of the two circles here, and finally by rotating by an angle γ about the new Z, δ_{33} here.

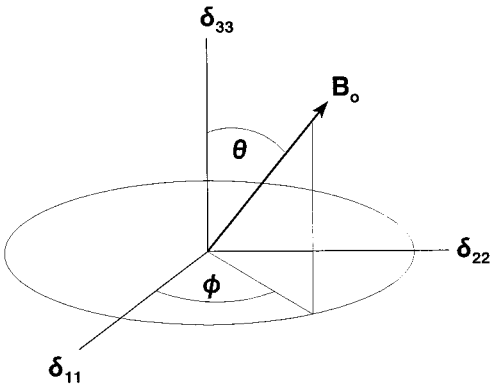

Figure 3. Orientation of the applied field, B_0, in the principal axis system of the chemical shift tensor.

By placing two homonuclear dilute spins adjacent to one another (e.g., by isotopic labeling), one obtains an isolated spin pair. In general, when the two coupled spins are not magnetically equivalent, there are four NMR transitions associated with each particular crystallite orientation.[12] The transition frequencies, ν_i, and relative intensities, P_i, of these transitions are

$$\nu_1 = \frac{1}{2}(\nu_A + \nu_B + D + A); \quad P_1 = 1 - \frac{B}{D} \quad (2a)$$

$$\nu_2 = \frac{1}{2}(\nu_A + \nu_B + D - A); \quad P_2 = 1 + \frac{B}{D} \quad (2b)$$

$$\nu_3 = \frac{1}{2}(\nu_A + \nu_B - D + A); \quad P_3 = 1 + \frac{B}{D} \quad (2c)$$

$$\nu_4 = \frac{1}{2}(\nu_A + \nu_B - D - A); \quad P_4 = 1 - \frac{B}{D} \quad (2d)$$

where

$$A = J_{iso} - R_{eff}(3\cos^2\zeta - 1)$$

$$B = J_{iso} + {}^1/_2 R_{eff}(3\cos^2\zeta - 1)$$

$$D = [(\nu_A - \nu_B)^2 + B^2]^{1/2}$$

In eq 2, ν_A and ν_B are the resonance frequencies of spins A and B, ζ is the angle between the applied magnetic field and

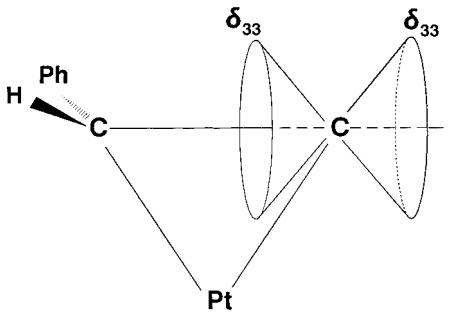

Figure 4. Possible orientations of δ_{33} about one of the olefinic carbons, as determined by the dipolar-chemical-shift technique. For clarity, the substituents about the olefinic carbon of interest have been omitted.

the dipolar vector $\mathbf{r}_{AB}$ (i.e., the olefinic C,C bond for the compounds investigated here), and R_{eff} is the effective dipolar coupling constant:

$$R_{eff} = R_{DD} - \Delta J/3 \quad (3)$$

The dipolar coupling constant, R_{DD}, which is dependent upon the inverse cube of the internuclear separation, is defined by

$$R_{DD} = \left(\frac{\mu_0}{4\pi}\right)\left(\frac{\hbar}{2\pi}\right)\gamma^2\langle r_{AB}{}^{-3}\rangle \quad (4)$$

where γ is the magnetogyric ratio and J_{iso} is the isotropic indirect spin−spin coupling, with an anisotropy of ΔJ.[12f] The angular brackets in the above equation indicate that the internuclear separation, and hence the observed dipolar coupling, is subject to motional averaging.[13]

In a powder sample, crystallites are oriented randomly in the applied magnetic field, resulting in the so-called powder pattern. For a given crystallite orientation, one will observe a doublet with a splitting which depends on the angle ζ and the magnitude of R_{eff}. The splitting observed when the applied field is parallel to a given principal component of the CS tensor allows the determination of the angle between this component and the dipolar vector, $\mathbf{r}_{AB}$.[14] However, because the dipolar vector is axially symmetric, the angle α, which defines the rotation of the CS tensor about this vector (see Figure 2), is not known, although the relative value of α for the two CS tensors is determined. The calculated spectrum is therefore invariant to simultaneous rotation of the two CS tensors about the dipolar vector. The sign of the dipolar splitting when the field is in the direction of δ_{33} is unknown, resulting in two possible solutions, an angle β and its complement. A calculated spectrum based on the dipolar-chemical-shift method therefore yields an infinite set of solutions, with δ_{33} oriented about two cones, as shown in Figure 4. Similarly, the calculated spectrum is invariant to the sign of the Euler angle γ. In some cases, molecular symmetry may be used to further elucidate the CS tensor orientation. For example, nuclei lying in a mirror plane must have two of their principal components in this plane. The orientation of CS tensors in closely related compounds, and the results of ab initio calculations[15] may also assist in the determination of CS tensor orientations.

If the two nuclei under consideration are related by a center of inversion, they will have identical CS tensors, i.e., the same principal components and orientations, resulting in an A_2 spin system.[11a] However, if the nuclei are crystallographically equivalent but magnetically nonequivalent, the resulting CS tensors will have the same principal components but different orientations. In such cases, the resulting powder spectrum may exhibit A_2, AB, and perhaps AX characteristics simultaneously, leading to a complex powder spectrum.[12c,16]

The principal components of a CS tensor may also be determined from the analysis of spinning sideband patterns of NMR spectra acquired under conditions of slow MAS, using the methods of Maricq and Waugh[17] or Herzfeld and Berger.[18] These techniques, which are based on the intensity of the sidebands, do not provide information on the orientation of the CS tensors. In the case of a homonuclear spin pair, the direct dipolar interaction is not completely removed by MAS,[17] and the line shapes of MAS sidebands are dependent on the relative orientations and magnitudes of the CS tensors.[12c,19] This effect, which has been explained using average Hamiltonian theory[17] and Floquet theory,[20] is proportional to the product of the instantaneous chemical shift difference and the direct dipolar or indirect spin−spin coupling. Hence, in suitable cases, investigation of spinning sidebands provides another method of determining the orientation of CS tensors.

2. Ab Initio Calculations of Chemical Shielding Tensors. Accurate first principles calculation of chemical shielding tensors is one of the most rigorous tests of computational techniques.[21] Such calculations are particularly daunting in the case of organometallic complexes, since all-electron calculations for heavy nuclei are computationally demanding,[22] and relativistic effects must be considered,[23] even for the shielding of the ligand nuclei.[24] The development of pseudopotentials, also known as effective core potentials (ECPs), has reduced the computational time by replacing the core electrons of heavy nuclei with parametrized functions which account for relativistic effects.[25] While their use is not recommended for the calculation of the magnetic properties of metal nuclei, acccurate shielding parameters for organometallic ligand nuclei have been achieved using ECPs for the heavy nuclei.[26] If structural modifications arising from vibrational motions are assumed to be small relative to the rigid molecule, then the shielding may be described in terms of a power series:[27]

$$\sigma_0(T) = \sigma_e + \sum_i \frac{\partial\sigma_e}{\partial q_i}\langle q_i\rangle^T + \sum_{ij}\frac{1}{2}\frac{\partial^2\sigma_e}{\partial q_i\,\partial q_j}\langle q_i q_j\rangle^T + \ldots \quad (5)$$

where $\sigma_0(T)$ is the shielding at temperature T, σ_e is the shielding at the rigid equilibrium geometry, and $q_{i,j}$ are the bond lengths or angles under consideration. Since the observed shielding will be that arising from the motionally averaged structure, a thorough theoretical investigation of the shielding entails the calculation of eq 5 at a wide range of bond lengths and angles, which is impractical for all but the smallest of molecules. However, a benefit of computational techniques is that, by varying one structural parameter while holding the remainder constant, the effect of changes to this parameter may be assessed. In this study, we will investigate $(\partial\sigma_{ii}/\partial r_{CC})\langle r_{CC}\rangle$, where r_{CC} is the olefinic C,C bond length.

Experimental Section

Compound **1**, *trans*-stilbene-α,β-$^{13}C_2$ (99.5% ^{13}C), was obtained from MSD Isotopes (Montreal, Canada) and used without further purification. Compound **2**, Pt(η^2-*trans*-stilbene-α,β-$^{13}C_2$)$(PPh_3)_2$, was prepared as described in the literature.[28]

Solid-state ^{13}C NMR spectra were obtained on Bruker MSL-200 (B_0 = 4.7 T) and AMX-400 (B_0 = 9.4 T) NMR spectrometers, operating at 50.32 and 100.62 MHz for ^{13}C nuclei, respectively. Cross-polarization (CP) under the Hartmann−Hahn match condition, with contact times of 5 ms, high-

TABLE 1: Calculated and Experimental Carbon Chemical Shift Tensors[a] of Some Olefinic Ligands and Their Pt(0) Complexes

	δ_{11}	δ_{22}	δ_{33}	δ_{iso}	Ω^b	κ^c
trans-stilbene						
calculated	232	124	51	136	181	−0.199
experimental	215	120	49	128	166	−0.145
$\partial\sigma_{ii}/\partial r_{CC}$ (ppm/Å)	−221	−156	−30	−135		
ethene						
calculated	259	121	21	134	238	−0.164
experimental[35]	234	120	24	126	210	−0.086
Pt(0)(*t*-stilbene)(PR_3)$_2$[d]						
calculated	109	68	54	77	55	−0.491
experimental	92	71	41	68	51	0.176
Pt(0)(ethene)(PR_3)$_2$[d]						
calculated	77	38	8	41	69	−0.130
experimental				39		

[a] See Experimental Section for details. Chemical shifts were calculated by taking the absolute shielding of TMS to be 188.1 ppm,[60] i.e., $\delta(\text{calc}) = 188.1 - \sigma(\text{calc})$. [b] $\Omega = \delta_{11} - \delta_{33}$. [c] $\kappa = 3(\delta_{22} - \delta_{iso})/\Omega$. [d] Calculated, R = CH_3; experimental, R = C_6H_5.

power proton decoupling, with ^{1}H 90° pulses of 2.8−3.8 μs, and recycle times of 100−120 s were used in acquiring all ^{13}C NMR spectra. Spectra were referenced to TMS by setting the high-frequency isotropic peak of an external adamantane sample to 38.57 ppm. MAS spectra were calculated using the program NMRLAB.[29] This program, mounted on an SGI Indy workstation, performed a powder averaging by sampling 10000 crystal orientations according to the Monte Carlo method. Spectra of stationary powder samples were calculated, from eq 2, using a program developed in this laboratory that incorporates the POWDER routine of Alderman et al.[30]

Calculation of the carbon CS tensors was performed on IBM RISC/6000 computers using the Gaussian 94 suite of programs.[31] These calculations used Becke's three-parameter hybrid functional[32] with the correlation functional of Lee−Yang−Parr[33] and GIAO[10] (B3LYP-GIAO).

The shielding tensors of the olefinic carbon nuclei of **1** were calculated with the 6-311+G(d) basis set (Table 1), using the experimental geometry[34] for the carbon skeleton and optimized (B3LYP/6-31G(d)) hydrogen parameters. To investigate the sensitivity of the CS tensor components to bond length extension, calculations were also performed on **1** with the geometry as described above, apart from the olefinic C,C bond length, which was increased in 0.01 Å increments to 1.36 Å. The first derivatives of the carbon shielding tensor components were determined by fitting the resulting data to a linear regression curve.

As a test of the computational techniques described above, calculations were also performed on ethene, its CS tensor having been fully characterized by both experimental[35] and theoretical[36] techniques. The molecular structure used for these calculations is that determined by Allen and Plyler from an IR study.[37]

To keep computational time within practical limits, calculations were performed on a model compound of **2**, Pt(*trans*-stilbene)(PMe_3)$_2$, **3**, also using B3LYP-GIAO, with a locally dense basis set[38] consisting of 6-311+G(d) for the olefinic carbon and adjacent proton and carbon atoms, 6-31G(d) for the remaining aromatic carbons on the stilbene moiety, 3-21G for the methyl groups and a modified Los Alamos ECP (LANL2DZ),[25b] as implemented by Gaussian 94, for platinum and phosphorus. The LANL2DZ ECP uses a "small core", which includes the 5s and 5p electrons in a contracted (8s6p3d)/[3s3p2d] basis set for platinum, whereas a contracted (3s3p)/[2s2p] basis set is used for phosphorus. The geometry of the heavy nuclei of **3** is based on the experimental geometry of the 4,4′-dinitro derivative of **2**, as reported by Baraban and McGinnety,[39] with trimethylphosphine groups replacing the triphenylphosphine groups. Because our NMR analysis of **2** yielded identical isotropic chemical shifts for the olefinic carbons, implying a molecule with local C_2 symmetry, average values of the relevant parameters from the experimental structure[39] were used to ensure C_2 symmetry, with coplanar platinum, phosphorus, and olefinic carbon atoms. The hydrogen parameters are those obtained from a geometry optimization of Pt(C_2H_4)(PMe_3)$_2$, **4**, as discussed below.

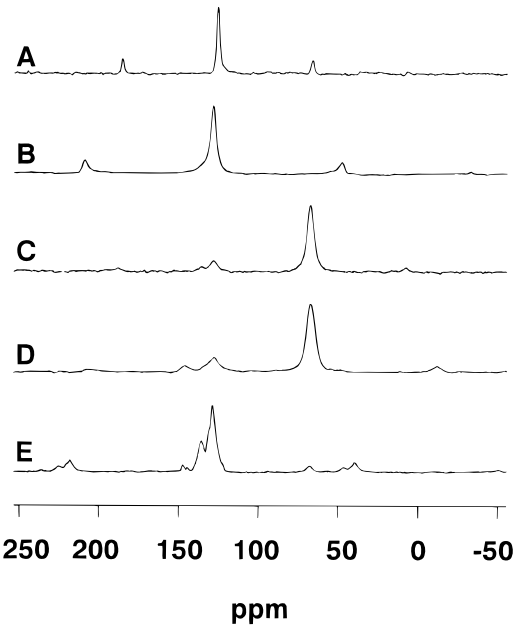

Figure 5. ^{13}C CP/MAS NMR spectra of *trans*-stilbene, **1**, at (A) ν_{rot} = 6 kHz and B_0 = 9.4 T and (B) ν_{rot} = 4 kHz and B_0 = 4.7 T. The line width of the isotropic peak is 120 Hz at 4.7 T and 150 Hz at 9.4 T. Traces C and D show the corresponding spectra for Pt(*trans*-stilbene)(PPh_3)$_2$, **2,** at 9.4 and 4.7 T, respectively, with ν_{rot} as for **1**. Trace E, the CP/MAS spectrum of an unlabeled sample of **2**, at 9.4 T and ν_{rot} = 8 kHz, illustrates that the peak at approximately 128 ppm in traces C and D arises from the natural abundance aromatic ^{13}C nuclei of the complex.

The olefinic carbon CS tensor of **4**, a model compound for Pt(C_2H_4)(PPh_3)$_2$, was also calculated using a locally dense basis set as described for **3**. Mirror symmetry in **4** was ensured by using the average geometry of the heavy nuclei of the triphenylphosphine derivative of **4**, as determined by X-ray crystallography.[40] The positions of the hydrogen atoms were determined by an ab initio DFT geometry optimization of **4** using a 6-31G(d) basis set.

Results and Discussion

CP/MAS NMR Spectra of *trans*-Stilbene-α,β-$^{13}C_2$, 1. The ^{13}C CP/MAS spectra of **1** are shown in Figure 5A,B. The observed isotropic chemical shift, 128 ppm, is typical of olefinic carbons[41] and is in agreement with the results of a solution study of **1**.[42] The crystal structure of **1**, determined by X-ray crystallography, shows that the monoclinic crystals (space group $P2_1/c$) consist of two crystallographically nonequivalent molecules lying at approximate inversion centers of the unit cell, one of which exhibits orientational disorder.[34,43] The molecules at the disordered site are related by an approximate 2-fold rotation about an axis joining the para carbons of the phenyl groups; this results in only a minor positional displacement of the olefinic carbons. The similar spectra at 9.4 and 4.7 T

indicate that the olefinic carbons of the crystallographically nonequivalent molecules have, within error, identical isotropic chemical shifts.

CP/MAS NMR Spectra of Pt(η^2-*trans*-stilbene-α,β-$^{13}C_2$)-(PPh_3)$_2$, 2. The ^{13}C CP/MAS NMR spectra of **2** are shown in Figure 5C,D. Comparison with the spectra of **1** shows that the isotropic carbon CS of the olefinic carbons is shifted to 68 ppm upon coordination to Pt(0), an increased shielding of 60 ppm. This compares to the increased shielding, relative to that of ethene,[35] of 89 ppm observed for Pt(C_2H_4)(PPh_3)$_2$;[44] comparable effects have also been reported in solution-state studies of Pt−olefin complexes.[3,4] The ^{13}C CP/MAS NMR spectra of **2** (Figure 5C,D) exhibit broad isotropic peaks, with widths of 350 Hz at 4.7 T and 500 Hz at 9.4 T, much broader than the 120 and 150 Hz line widths observed for the corresponding isotropic peaks of **1**. Indirect and direct dipolar coupling interactions with the protons should be removed by decoupling. However, Chaloner and co-workers have reported $^2J(^{31}P,^{13}C)$ of 20.5−26.7 and 4.7−5.3 Hz for the two ^{31}P nuclei of **2**.[4b] Although these authors do not report $^1J(^{195}Pt,^{13}C)$, this value is expected to be similar to that obtained for Pt(C_2H_4)(PPh_3)$_2$, 196 Hz.[45] Hence, the observed line broadening is ascribed primarily to spin−spin coupling interactions with ^{195}Pt (spin $^1/_2$, natural abundance, 33.8%) and ^{31}P; the difference in the isotropic chemical shift of the two ^{13}C nuclei is thought to be negligible. Mechanisms for line broadening in solid-state MAS NMR have been discussed in detail.[46]

The ^{13}C CP/MAS NMR spectra of **2** contain a weak peak at approximately 128 ppm (Figure 5C,D). Although it appears to be due to unreacted *trans*-stilbene, the ^{13}C NMR spectrum of an unlabeled sample of **2** (Figure 5 E) contains an intense peak at $\delta = 128$ ppm. Thus, the weak peak at 128 ppm shown in Figure 5C,D arises from the natural abundance aromatic ^{13}C nuclei of **2**—not surprising for a molecule containing a total of eight phenyl groups.

Figure 6 shows the experimental and calculated CP/MAS spectra of **2** obtained at various spinning rates (ν_{rot}). The calculated spectra (Figure 6A,C,E) were generated using the parameters obtained from an analysis of the stationary sample (vide infra). The high-frequency portions of the experimental spectra are complicated by the peaks arising from natural abundance aromatic ^{13}C nuclei; however, the spinning sidebands of the olefinic carbons are well-resolved at lower frequencies. The asymmetry in the first-order spinning sidebands of the spectrum obtained with $\nu_{rot} = 2$ kHz (Figure 6F) support the conclusion that the spin pairs are crystallographically equivalent but magnetically nonequivalent, since a single transition is expected for the sidebands of an A_2 spin system.[19] The splitting in the isotropic peak (Figure 6E) is also a consequence of the magnetically nonequivalent nuclei. This effect is unresolved in the experimental spectrum, probably because of broadening due to $^1J(^{195}Pt,^{13}C)$ and $^2J(^{31}P,^{13}C)$, which are not included in the calculation of the theoretical spectrum. The isotropic peaks of the experimental spectra (Figure 6B,D,F) are not affected significantly by ν_{rot}, supporting the contention that the line broadening arises from unresolved $^1J(^{195}Pt,^{13}C)$ and $^2J(^{31}P,^{13}C)$.

Olefinic Carbon Chemical Shift Tensors in *trans*-Stilbene. The ^{13}C NMR spectra of a stationary sample of **1** are shown in Figure 7 with the corresponding calculated spectra. The two olefinic ^{13}C nuclei in each of the two molecules in the unit cell of **1** are related by a center of inversion,[34] constituting an A_2 spin system. Since the two crystallographically nonequivalent molecules have, within error, identical isotropic carbon chemical shifts, the spectra consist of two dipolar subspectra, as expected for an A_2 spin system. In contrast, slightly different nitrogen CS tensors were observed for *trans*-azobenzene,[47] which is isostructural with **1** and exhibits the same type of disorder;[48] this may be due to the greater sensitivity of the nitrogen nucleus to subtle structural differences.

A single set of CS parameters was assumed for the two sites of **1**. The agreement between the observed and calculated ^{13}C NMR spectra (Figure 7) indicates that this is a reasonable assumption. Analyses of these spectra yield the following

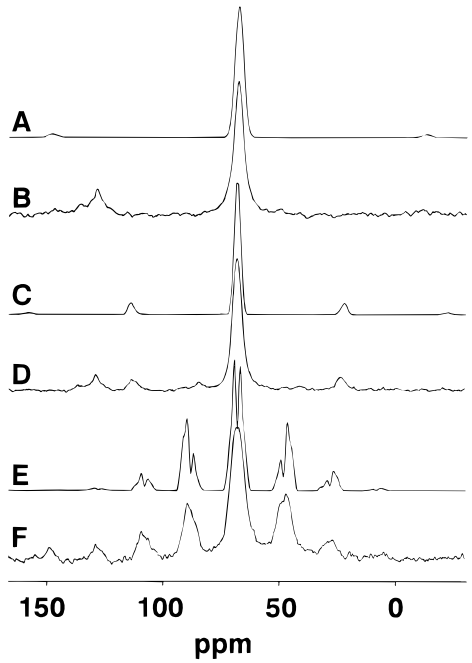

Figure 6. Calculated (A) and experimental (B) CP/MAS spectra of **2** at 9.4 T with $\nu_{rot} = 8$ kHz. Traces C and D are the corresponding spectra with $\nu_{rot} = 4.5$ kHz, and traces E and F correspond to $\nu_{rot} = 2$ kHz. The additional peaks appearing at the higher frequencies of the experimental spectra are attributed to the natural abundance aromatic ^{13}C nuclei of **2**.

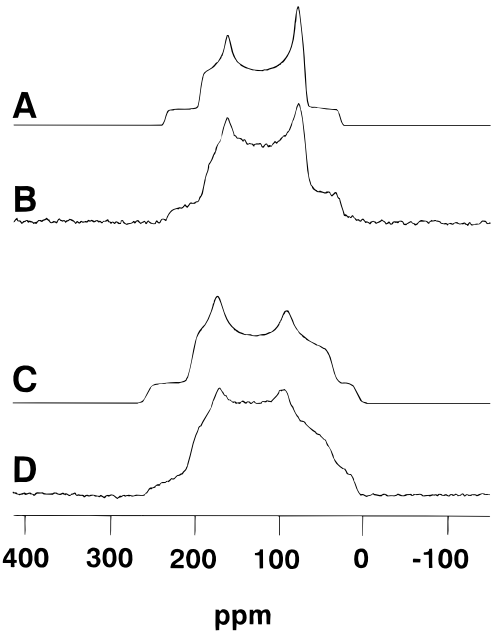

Figure 7. Calculated (A) and experimental (B) ^{13}C NMR spectra of a stationary sample of *trans*-stilbene, **1**, at $B_0 = 9.4$ T. Traces C and D are the corresponding ^{13}C NMR spectra of a stationary sample of **1** at $B_0 = 4.7$ T.

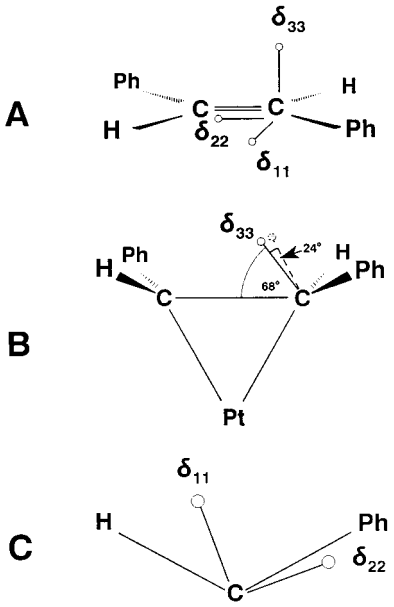

Figure 8. (A) Orientation of the carbon CS tensor of **1**. (B) Orientation of δ_{33} in **2**. This component is oriented 68° from the olefinic C,C bond and lies 24° off the plane defined by the platinum and the two olefinic carbons. (C) The H−C−C_{ipso} plane of **2** is shown, illustrating the orientation of δ_{11} and δ_{22}. Both components are approximately in this plane.

principal components for the olefinic carbon CS tensors of **1**: $\delta_{11} = 215$, $\delta_{22} = 120$, and $\delta_{33} = 49$ ppm, each with an uncertainty estimated to be less than 2 ppm. Since it is known that the most shielded component, δ_{33}, of olefinic carbon CS tensors is always approximately perpendicular to the plane defined by the olefinic carbon and its substituents,[35,49] this component was fixed during the search for the "best-fit" line shape. The final calculated spectra were obtained using the following orientation: the least shielded component, δ_{11}, is nearly perpendicular to the olefinic C,C bond and lies in the molecular plane. More specifically, the angle between δ_{11} and the ^{13}C,^{13}C dipolar vector is 85 ± 5°. This places the intermediate component, δ_{22}, approximately along the C,C bond. This orientation, illustrated in Figure 8A, is similar to that reported for the olefinic carbons of ethene[35] and *trans*-2-butene.[36]

This CS tensor may be understood in terms of Ramsey's theory, which partitions the observed shielding into diamagnetic and paramagnetic contributions.[50] The diamagnetic contribution is positive, leading to greater shielding, whereas the paramagnetic contribution invariably is negative, leading to deshielding. In general, the diamagnetic contribution shows a fairly weak orientation dependence. For example, the diamagnetic shielding perpendicular to the molecular plane of ethene is estimated to be 337 ppm while the component in the molecular plane, perpendicular to the C,C bond, is 331 ppm. The remaining component, parallel to the C,C bond, is 280 ppm.[51] On the other hand, the paramagnetic contribution to the shielding tensor components is often strongly dependent on orientation. It involves the mixing of the ground- and excited-state wave functions connected by magnetic-dipole-allowed transitions, which correspond to excitations between molecular orbital levels having nonzero matrix elements of the *x*, *y*, and *z* components of the angular momentum. Because the *z* component of the electron orbital angular momentum operators have the same symmetry as rotation operators about *x*, *y*, and *z*, they connect orbitals such that charge appears to rotate.[50b,52] To a first approximation, the electronic properties of the olefinic carbons of **1** will be comparable to those of ethene. Since there are no low-energy transitions corresponding to rotation about the axis perpendicular to the molecular plane, there is little deshielding in this direction. However, mixing of π and σ^* orbitals, resulting from rotation about the axis in the molecular plane, perpendicular to the C,C bond, contributes to the deshielding observed along this axis. Similarly, mixing of the σ and π^* orbitals, resulting from rotation about the C,C bond, contributes to the deshielding observed in the direction parallel to this bond.

The accepted olefinic C,C bond length of *trans*-stilbene, **1**, as determined by X-ray diffraction, is 1.326 Å,[34] less than the computed value of 1.35−1.36 Å.[53] The unusually short experimental bond length has been attributed to large-amplitude motion of the phenyl groups,[54] although it has also been suggested that the experimental bond length may be misleading,[53b] due to the disorder in the crystal.[34] This bond length may be estimated from the measured ^{13}C,^{13}C dipolar coupling constant, which is related to the inverse cube of the internuclear separation. In principle, one should consider the contribution of Δ^1J to R_{eff} (eq 3). This value, unavailable for **1**, is estimated to be approximately 90 Hz in ethene-$^{13}C_2$,[55] and is less than 30 Hz in benzene-$^{13}C_6$.[56] Hence, the contribution to R_{eff} from $\Delta J/3$ is thought to be negligible, resulting in $R_{eff} \approx R_{DD}$ and allowing the calculation of r_{CC}. The ^{13}C,^{13}C dipolar coupling constant used in the calculated spectra shown in Figure 7 is 2.8 ± 0.2 kHz, corresponding to $r_{CC} = 1.39 \pm 0.03$ Å, which is longer than the experimental value.[34] This is probably a consequence of motional averaging of the ^{13}C,^{13}C dipolar interaction.[12c,13] The olefinic C,C bond lengths for the two types of molecules present in the unit cell differ by 0.004 Å, which corresponds to a difference of only 30 Hz in their respective R_{DD} values, negligible compared to the uncertainty in R_{eff}. Hence, only one value of the ^{13}C,^{13}C dipolar coupling constant was used in the line shape calculations described above.

Table 1 lists the calculated values of the CS tensors of **1**, ethene, and their corresponding Pt(0)(PMe_3)$_2$ complexes. The calculated orientations of the CS tensors of **1** and ethene are in exact agreement with experiment, while the principal components, particularly at higher frequency, are deshielded slightly compared to experimental values. The calculated principal components of the CS tensor for ethene are comparable to the results of Orendt and co-workers, calculated using IGLO (individual gauge for localized orbitals).[36] Given that solid-state experimental data are compared with the results of calculations performed on rigid, gas-phase molecules, the agreement may be considered excellent. These results also show that agreement with experiment improves as the shielding increases, not unusual for DFT calculations.[21e] This reflects the difficulty of accurately calculating the paramagnetic contribution to the shielding, as well as the sensitivity to vibrational and intermolecular effects of this contribution.[27a]

Table 1 also lists the first derivatives of the calculated shielding of **1** with respect to bond extension. All three components have negative derivatives; that is, the shielding decreases with increasing bond length. This general observation has been made from NMR investigations of isotope effects on chemical shifts and also from variable temperature studies of NMR chemical shifts.[27a] The calculated isotropic first derivative of the shielding, −135 ppm/Å, is slightly smaller than the approximately −177 ppm/Å derivative calculated for ethene using a similar basis set.[27b] These calculations demonstrate the sensitivity of the chemical shielding to the molecular structure.

Olefinic Carbon Chemical Shift Tensor for Pt(η^2-*trans*-stilbene)(PPh_3)$_2$. Carbon-13 NMR spectra of a stationary

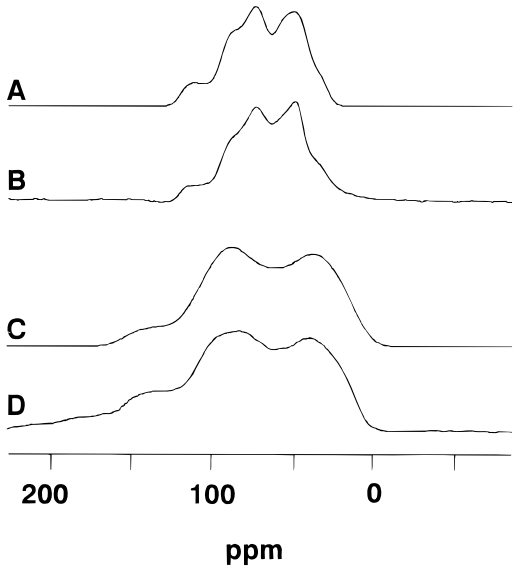

Figure 9. Calculated (A) and experimental (B) ^{13}C NMR spectra of a stationary sample of Pt(*trans*-stilbene)$(PPh_3)_2$, **2**, at $B_0 = 9.4$ T. Traces C and D are the corresponding spectra at $B_0 = 4.7$ T.

sample of **2** are shown in Figure 9, B and D, respectively. For comparison, the corresponding "best-fit" calculated spectra are shown in Figure 9, A and C. The calculated spectra were generated by assuming the CS tensors of the two carbons are related by a C_2 axis (i.e., $\alpha = 0, 180°$) using the following parameters: $\delta_{11} = 92 \pm 2$ ppm, $\delta_{22} = 71 \pm 2$ ppm, $\delta_{33} = 41 \pm 2$ ppm, $R_{eff} = 2.5 \pm 0.2$ kHz, $\beta = 112 \pm 3°$, and $\gamma = 25 \pm 5°$. The complement of $\beta = 112°$, 68°, will also yield the same calculated spectra, as will $\gamma = -25°$. The two cones corresponding to $\beta = 112°$and 68° are illustrated in Figure 4. To fix the orientation of δ_{33} in the molecular axis system, we turn to theoretical calculations. The calculated orientation of δ_{33} for the olefinic carbons of Pt(η^2-*trans*-stilbene)$(PMe_3)_2$, **3**, corresponds to $\beta = 73°$, in good agreement with experiment; δ_{33} lies 24° out of the C−Pt−C plane as illustrated in Figure 8B. A similar orientation, $\beta = 66°$, was calculated for the olefinic carbon tensor of Pt(η^2-ethene)$(PMe_3)_2$, **4**; however, the presence of a mirror plane, absent in **3**, fixes δ_{33} in the C−Pt−C plane. Given the good agreement between the experimental value of β and the theoretical values calculated for **3** and **4**, it is reasonable to assume that δ_{33} for the olefinic carbons of Pt(η^2-*trans*-stilbene)$(PPh_3)_2$ must lie close to the C−Pt−C plane as shown in Figure 8B. With δ_{33} oriented 24° out of the C−Pt−C plane, the experimental values of γ, ±25°, imply that δ_{22} is oriented either toward the ipso carbon of the stilbene phenyl ring (see Figure 8C) or toward the olefinic hydrogen. Since theoretical calculations of the carbon shielding tensor for **3** support the former general orientation of δ_{22}, the orientation of our combined experimental, theoretical olefinic carbon shielding tensor for Pt(η^2-*trans*-stilbene)$(PPh_3)_2$, **2**, is summarized in Figure 8B,C.

Comparison of the carbon CS tensors of **1** and **2** (Table 1) reveals significant differences in the magnitudes of the principal components of their carbon CS tensors. Upon coordination with Pt(0), the span of the olefinic carbon CS tensor is reduced from 166 to 51 ppm, primarily due to changes in δ_{11} and δ_{22}. The lack of symmetry at the olefinic carbon nuclei of Pt(η^2-*trans*-stilbene)$(PPh_3)_2$, **2**, makes a direct comparison of their orientations difficult. However, we note that in the complex the carbon CS tensor apparently remains oriented in the plane described by the olefinic carbon and its substituents (Figure 8C).

The geometry about the olefinic carbons of Pt(0)−olefin complexes has been qualitatively described in terms of the model proposed by Dewar, Chatt, and Duncanson,[57] in which donation of electron density from the Pt to the π^* antibonding orbitals of the olefin results in a weakening, and hence a lengthening, of the olefinic C,C bond, as well as to increased electron density in the olefin−substituent bond. The bond pair/bond bond repulsion resulting from this increased electron density is thought to be responsible for the bending of the substituents away from the platinum.[1] The orientation of the carbon CS tensor for **2** reflects the geometry about the olefinic carbons. The deshielded components, δ_{11} and δ_{22}, remain in the plane defined by the olefinic carbon and its two substituents, with δ_{33} perpendicular to this plane.

The model proposed by Dewar, Chatt, and Duncanson[57] also offers a qualitative explanation for the changes in the magnitude of the CS tensor components upon coordination to Pt(0). The deshielding in the directions of δ_{11} and δ_{22} in the olefin results primarily from mixing of σ and π^* as well as π and σ^* orbitals. Hence, donation of electron density to the π^* orbitals of the olefinic carbons of the complex will reduce this mixing, resulting in the observed increased shielding. The orientation of the substituents about the olefinic carbons of metal complexes may be described as being intermediate between that of an olefin and an alkane, the absence of low-lying excited electronic states in the latter resulting in a small span for the CS tensor of its carbons.[52] The span of the CS tensor of **2**, 51 ppm, is indeed intermediate between that of the olefin, 166 ppm, and of ethane, 7 ppm.[58]

A dipolar coupling of 2.5 ± 0.2 kHz was used to calculate the spectra of **2** (Figure 9), which, again assuming ΔJ is negligible, corresponds to a C,C bond length of 1.45 ± 0.03 Å. This compares to the 1.416 Å reported for the olefinic C,C bond of 4,4′-dinitro-*trans*-stilbene[bis(triphenylphosphine)]platinum.[39] As for **1**, motional averaging probably results in a longer value of r_{CC}.[13]

The orientation of the calculated CS tensor of **3** corresponds to Euler angles of $\beta = 73°$ and $\gamma = 45°$, compared to experimental values, for **2**, of 68 ± 3° and 25 ± 5°, respectively. Accurately calculating the orientation of a CS tensor with a small span, such as **2**, is particularly challenging, since the CS tensor is relatively insensitive to small changes in orientation. As well as the neglect of inter- and intramolecular effects, discrepancies in the calculated CS tensor may result from the uncertain geometry of **2**. Calculations revealed that the CS tensor orientation is very sensitive to the geometry about the olefinic carbons. An ab initio geometry optimization of **2** is impractical and would not necessarily yield the geometry prevailing in the solid state. Unfortunately, attempts to grow single crystals of **2** suitable for X-ray diffraction measurements have been unsuccessful to date. In principle, a computational technique should not be assessed solely from the results at one level of theory, since agreement with experiment may be fortuitous. Unfortunately, for a molecule of this size, it is not practical at this time to perform calculations at various levels of theory or with different ECPs. However, other workers have shown that calculated CS tensor components converge at a comparable level of theory.[10c,21,59]

Despite the difficulties inherent in the calculation of CS tensors for large molecules, we believe that the combination of experimental and theoretical methods can lead to considerable insight into carbon CS tensors in transition metal−olefin complexes. When analysis of single crystals is impractical, the computational techniques, along with the constraints imposed

by the experimental results, offer the most information about the CS tensor. The magnitudes of the principal components are determined, and we are able to propose an orientation in the molecular framework.

Conclusions

We have shown that the olefinic carbon chemical shift tensors of *trans*-stilbene change dramatically on coordination to platinum-(0). In particular, the span of the carbon chemical shift tensor is considerably reduced in the Pt(0) complex, primarily because of changes to δ_{11} and δ_{22}. The orientation of the carbon CS tensor of the complex is sensitive to the orientation of the substituents about the olefinic carbons. Since data on carbon chemical shift tensors of organometallic compounds are scarce, possible extensions of the work outlined above will be of general interest. We have also shown that these tensor components may be calculated with reasonable accuracy using DFT and ECPs, even for large molecules, making this technique a valuable tool for assigning the CS tensor orientations of molecules analyzed from powder samples.

Acknowledgment. We are very grateful to Mr. Devin Latimer for preparing the platinum complexes used in this study and to Dr. Klaus Eichele, Ms. Myrlene Gee, Mr. Scott Kroeker, and Mr. Rob Schurko for many helpful suggestions. We are also grateful to Professor Ted Schaefer of the University of Manitoba, for allowing the use of his computer for some of the theoretical calculations reported herein, to Dr. Boqin Sun, Professor Malcolm H. Levitt, and Professor Aatto Laaksonen, for providing various simulation programs, and to Dr. Tom Stringfellow, for his advice on the computational aspects of this work. R.E.W. wishes to thank the Natural Sciences and Engineering Research Council (NSERC) of Canada for operating and equipment grants and the Canada Council for a Killam Research Fellowship. G.M.B. acknowledges NSERC, the Walter C. Sumner Foundation, and the Izaak Walton Killam Trust for postgraduate scholarships. All solid-state NMR spectra were recorded at the Atlantic Region Magnetic Resonance Centre, which is also supported by NSERC.

References and Notes

(1) Hartley, F. R. In *Comprehensive Organometallic Chemistry*; Wilkinson, G., Ed.; Pergamon Press: Oxford, 1982; Vol. 6, p 471.

(2) For continuity, the term "olefinic" will be used to describe the olefinic carbons of the free ligands and the corresponding atoms in the complex, although in the latter case this does not conform to a strict definition of the term.

(3) Mann, B. E.; Taylor, B. F. *^{13}C NMR Data for Organometallic Compounds*; Academic Press: London, 1981.

(4) (a) Chisholm, M. H.; Clark, H. C.; Manzer, L. E.; Stothers, J. B. *J. Am. Chem. Soc.* **1972**, *94*, 5087. (b) Chaloner, P. A.; Davies, S. E.; Hitchcock, P. B. *Polyhedron* **1997**, *16*, 765.

(5) Wallruff, G. M. Ph.D. thesis, University of Utah, 1985. Cf.: Duncan, T. M. *Principal Components of Chemical Shift Tensors: A Compilation*, 2nd ed.; Farragut Press: Chicago, 1994.

(6) Huang, Y.; Gilson, D. F. R.; Butler, I. S. *J. Chem. Soc., Dalton Trans.* **1992**, 2881.

(7) Ding, S.; McDowell, C. A. *Chem. Phys. Lett.* **1997**, *268*, 194.

(8) Gay, I. D.; Young, G. B. *Organometallics* **1996,** *15*, 2264.

(9) Wang, J.; Ellis, P. D. *J. Am. Chem. Soc.* **1991**, *113*, 9675.

(10) (a) Ditchfield, R. *Mol Phys.* **1974**, *27*, 789. (b) Wolinski, K.; Hinton, J. F.; Pulay, P. *J. Am. Chem. Soc.* **1990**, *112*, 8251. (c) Rauhut, G.; Puyear, S.; Wolinski, K.; Pulay, P. *J. Phys. Chem.* **1996**, *100*, 6310.

(11) (a) Haeberlen, U. In *Advances in Magnetic Resonance*, Supplement 1; Waugh, J. S., Ed.; Academic Press: New York, 1976. (b) Schmidt-Rohr, K.; Spiess, H. W. *Multidimensional Solid-State NMR and Polymers*; Academic Press: London, 1994.

(12) (a) Power, W. P.; Wasylishen, R. E. *Ann. Rep. NMR Spectrosc.* **1991**, *23*, 1. (b) van Willigen, H.; Griffin, R. G.; Haberkorn, R. A. *J. Chem. Phys.* **1977**, *67*, 5855. (c) Zilm, K. W.; Grant, D. M. *J. Am. Chem. Soc.* **1981**, *103*, 2913. (d) Curtis, R. D.; Hilborn, J. W.; Wu, G.; Lumsden, M. D.; Wasylishen, R. E.; Pincock, J. A. *J. Phys. Chem.* **1993**, *97*, 1856. (e) Lumsden, M. D.; Wu, G.; Wasylishen, R. E.; Curtis, R. D. *J. Am. Chem. Soc.* **1993**, *115*, 2825. (f) Wasylishen, R. E. In *Encyclopedia of Nuclear Magnetic Resonance*; Grant, D. M.; Harris, R. K., Eds.; John Wiley and Sons: Chichester, 1996; p 1685.

(13) Ishii, Y.; Terao, T.; Hayashi, S. *J. Chem. Phys.* **1997**, *107*, 2760.

(14) Eichele, K.; Wasylishen, R. E. *J. Magn. Reson.* **1994**, *106A*, 46.

(15) Facelli, J. C. In *Encyclopedia of Nuclear Magnetic Resonance*; Grant, D. M.; Harris, R. K., Eds.; John Wiley and Sons: Chichester, 1996; p 4327.

(16) Lumsden, M. D.; Wasylishen, R. E.; Britten, J. F. *J. Phys. Chem.* **1995**, *99*, 16602.

(17) Maricq, M. M.; Waugh, J. S. *J. Chem. Phys.* **1979**, *70*, 3300.

(18) Herzfeld, J.; Berger, A. E. *J. Chem. Phys.* **1980**, *73*, 6021.

(19) (a) Wu, G.; Wasylishen, R. E. *J. Magn. Reson.* **1993**, *102A*, 183. (b) Wu, G.; Wasylishen, R. E. *J. Chem. Phys.* **1993**, *99*, 6321. (c) Wu, G.; Sun, B.; Wasylishen, R. E.; Griffin, R. G. *J. Magn. Reson.* **1997**, *124*, 366. (d) Dusold, S.; Klaus, E.; Sebald, A.; Bak, M.; Nielsen, N. C. *J. Am. Chem. Soc.* **1997**, *119*, 7121.

(20) (a) Schmidt, A.; Vega, S. *J. Chem. Phys.* **1992**, *96*, 2655. (b) Nakai, T.; McDowell, C. A. *J. Chem. Phys.* **1992**, *96*, 3452.

(21) (a) Webb, G, A. *Nuclear Magnetic Shieldings and Molecular Structure*; Tossell, J. A., Ed.; Kluwer Academic Publishers: Dordrecht, 1993. (b) Chesnut, D. B. *Ann. Rep. NMR Spectrosc.* **1994**, *29*, 71. (c) Gauss, J. *Ber. Bunsen-Ges. Phys. Chem.* **1995**, *99*, 1001. (d) de Dios, A. C. *J. Prog. NMR Spectrosc.* **1996**, *29*, 229. (e) Jameson, C. J. In *Nuclear Magnetic Resonance—A Specialist Periodical Report*; Webb, G. A., Ed.; Royal Society of Chemistry: Cambridge, Great Britain, 1997; Vol. 26 and previous volumes in this annual series.

(22) For a discussion of shielding calculations in organometallic complexes, see: Frenking, G.; Pidun, U. *J. Chem. Soc., Dalton Trans.* **1997**, 1653.

(23) (a) Pyykkö, P. *Chem. Rev.* **1988**, *88*, 563. (b) Li, J.; Schreckenbach, G.; Ziegler, T. *Inorg. Chem.* **1995**, *34*, 3245.

(24) (a) Kaupp, M.; Malkin, V. G.; Malkina, O. L.; Salahub, D. R. *J. Am. Chem. Soc.* **1995**, *117*, 1851. (b) Kaupp, M.; Malkina, O. L.; Malkin, V. G. *J. Chem. Phys.* **1997**, *106*, 9201.

(25) (a) Stevens, W. J.; Basch, H.; Krauss, M. *J. Chem. Phys.* **1984**, *81*, 6026. (b) Hay, P. J.; Wadt, W. R. *J. Chem. Phys.* **1985**, *82*, 270, 299. (c) Wadt, W. R.; Hay, P. J. *J. Chem. Phys.* **1985**, *82*, 284. (d) Hurley, M. M.; Pacios, L. F.; Christiansen, P. A.; Ross, R. B.; Ermler, W. C. *J. Chem. Phys.* **1986**, *84*, 6840. (e) Andrae, D.; Häussermann, U.; Dolg, M.; Stoll, H.; Preuss, H. *Theor. Chim. Acta* **1990**, *77*, 123. (f) Wallace, N. M.; Blaudeau, J. P.; Pitzer, R. M. *Int. J. Quantum Chem.* **1991**, *40*, 789. (g) Wittborn, C.; Wahlgren, U. *Chem. Phys.* **1995**, *201*, 357. (h) Russo, T. V.; Martin, R. L.; Hay, P. J. *J. Phys. Chem.* **1995**, *99*, 17085.

(26) (a) Kaupp, M.; Malkin, V. G.; Malkina, O. L.; Salahub, D. R. *Chem. Phys. Lett.* **1995**, *235*, 382. (b) Kaupp, M.; Malkin, V. G.; Malkina, O. L.; Salahub, D. R. *Chem. Eur. J.* **1996**, *2*, 24. (c) Kaupp, M. *Chem. Ber.* **1996**, *129*, 527. (d) Kaupp, M. *Chem. Ber.* **1996**, *129*, 535. (e) Schreckenbach, G. Ph.D. Thesis, University of Calgary, 1996.

(27) (a) Jameson, C. J.; Osten, H. J. *Ann. Rep. NMR Spectrosc.* **1986**, *17*, 1. (b) Chesnut, D. B.; Wright, D. W. *J. Comput. Chem.* **1991**, *12*, 546.

(28) Chatt, J.; Shaw, B. L.; Williams, A. A. *J. Chem. Soc.* **1962**, 3269.

(29) Sun, B.; Griffin, R. G. Unpublished results.

(30) Alderman, D. W.; Solum, M. S.; Grant, D. M. *J. Chem. Phys.* **1986**, *84*, 3717.

(31) Gaussian 94, Revision B.2: Frisch, M. J.; Trucks, G. W.; Schlegel, H. B.; Gill, P. M. W.; Johnson, B. G.; Robb, M. A.; Cheeseman, J. R.; Keith, T.; Petersson, G. A.; Montgomery, J. A.; Raghavachari, K.; Al-Laham, M. A.; Zakrzewski, V. G.; Ortiz, J. V.; Foresman, J. B.; Cioslowski, J.; Stefanov, B. B.; Nanayakkara, A.; Challacombe, M.; Peng, C. Y.; Ayala, P. Y.; Chen, W.; Wong, M. W.; Andres, J. L.; Replogle, E. S.; Gomperts, R.; Martin, R. L.; Fox, D. J.; Binkley, J. S.; Defrees, D. J.; Baker, J.; Stewart, J. P.; Head-Gordon, M.; Gonzalez, C.; Pople, J. A. Gaussian, Inc., Pittsburgh, PA, 1995.

(32) Becke, A. D. *J. Chem Phys.* **1993**, *98*, 5648.

(33) (a) Lee, C.; Yang, W.; Parr, R. G. *Phys. Rev.* **1988**, *B37*, 785. (b) Miehlich, B.; Savin, A.; Stoll, H.; Preuss, H. *Chem. Phys. Lett.* **1989**, *157*, 200.

(34) Bouwstra, J. A.; Schouten, A.; Kroon, J. *Acta Crystallogr.* **1984**, *C40*, 428.

(35) Zilm, K. W.; Conlin, R. T.; Grant, D. M.; Michl, J. *J. Am. Chem. Soc.* **1980**, *102*, 6672.

(36) Orendt, A. M.; Facelli, J. C.; Beeler, A. J.; Reuter, K.; Horton, W. J.; Cutts, P.; Grant, D. M.; Michl, J. *J. Am. Chem. Soc.* **1988**, *110*, 3386.

(37) Allen, H. C.; Plyler, E. K. *J. Am. Chem. Soc.* **1958**, *80*, 2673.

(38) (a) Chesnut, D. B.; Moore, K. D. *J. Comput. Chem.* **1989**, *10*, 648. (b) Chesnut, D. B.; Rusiloski, B. E.; Moore, K. D.; Egolf, D. A. *J. Comput. Chem.* **1993**, *14*, 1364.

(39) Baraban, J. M.; McGinnety, J. A. *Inorg. Chem.* **1974**, *13*, 2864.

(40) Cheng, P.-T.; Nyburg, S. C. *Can. J. Chem.* **1972**, *50*, 912.

(41) (a) Stothers, J. B. *Carbon-13 NMR Spectroscopy*; Academic Press: New York, 1972. (b) Duncan, T. M. *Principal Components of Chemical Shift Tensors: a Compilation*, 2nd ed.; Farragut Press: Chicago, 1994.

(42) Hansen, P. E.; Poulsen, O. K.; Berg, A. *Org. Magn. Reson.* **1976**, *8*, 632.

(43) (a) Finder, C. J.; Newton, M. G.; Allinger, N. L. *Acta Crystallogr.* **1974**, *B30*, 411. (b) Bernstein, J. *Acta Crystallogr.* **1975**, *B31*, 1268. (c) Hoekstra, A.; Meertens, P.; Vos, A. *Acta Crystallogr.* **1975**, *B31*, 2813.

(44) Unpublished results from this laboratory.

(45) Wrackmeyer, B. *Z. Naturforsch.* **1997**, *52B*, 1019.

(46) (a) Pausak, S.; Tegenfeldt, J.; Waugh, J. S. *J. Chem. Phys.* **1974**, *61*, 1338. (b) VanderHart, D. L.; Earl, W. L.; Garroway, A. N. *J. Magn. Reson.* **1981**, *44*, 361. (c) Alla, M.; Lippmaa, E. *Chem. Phys. Lett.* **1982**, *87*, 30. (d) Hemminga, M. A.; De Jager, P. A.; Krüse, J.; Lamerichs, R. M. J. N. *J. Magn. Reson.* **1987**, *71*, 446.

(47) Wasylishen, R. E.; Power, W. P.; Penner, G. H.; Curtis, R. D. *Can. J. Chem.* **1989**, *67*, 1219.

(48) Harada, J.; Ogawa, K.; Tomado, S. *Acta Crystallogr.* **1997**, *B53*, 662.

(49) (a) Spiess, H. W. *NMR: Basic Princ. Prog.* **1978**, *15*, 55. (b) Wolff, E. K.; Griffin, R. G.; Waugh, J. S. *J. Chem. Phys.* **1977**, *67*, 2387. (c) Mehring, M. *Principles of High-Resolution NMR in Solids*; Springer-Verlag: Berlin, 1983; Chapter 7. (d) Veeman, W. S. *Prog. NMR Spectrosc.* **1984**, *16*, 193.

(50) (a) Ramsey, N. F. *Phys. Rev.* **1950**, *78*, 699. (b) Jameson, C. J.; Mason, J. In *Multinuclear NMR*; Mason, J., Ed.; Plenum Press: New York, 1987; Chapter 3. (c) Schreckenbach, G.; Dickson, R. M.; Ruiz-Morales, Y.; Ziegler, T. In *Chemical Applications of Density-Functional Theory*; ACS Symposium Series 629; Laird, B. B., Ross, R. B., Ziegler, T., Eds.; American Chemical Society: Washington, DC, 1996; p 328.

(51) Zilm, K. W.; Duchamp, J. C. *Nuclear Magnetic Shieldings and Molecular Structure*; Tossell, J. A., Ed.; Kluwer Academic Publishers: Dordrecht, 1993.

(52) (a) Jameson, C. J.; Gutowsky, H. S. *J. Chem. Phys.* **1964**, *40*, 1714. (b) Grutzer, J. B. In *Recent Advances in Organic NMR Spectroscopy*; Lambert, J. B., Rittner, R., Eds.; Norell Press: Landisville, NJ, 1987; Chapter 2.

(53) (a) Molina, V.; Merchán, M.; Roos, B. O. *J. Phys. Chem. A* **1997**, *101*, 3478. (b) Choi, C. H.; Kertesz, M. *J. Phys. Chem. A* **1997**, *101*, 3823.

(54) (a) Saito, K.; Ikemoto, I. *Physica B* **1996**, *219 & 220*, 417. (b) Saito, K.; Ikemoto, I. *Bull. Chem. Soc. Jpn.* **1996**, *69*, 909. (c) Ogawa, K.; Harada, J.; Tomoda, S. *Acta Crystallogr.* **1995**, *B51*, 240. (d) Ogawa, K.; Sano, T.; Yoshimura, S.; Takeuchi, Y.; Toriumi, K. *J. Am. Chem. Soc.* **1992**, *114*, 1041.

(55) Diehl, P.; Sykora, S.; Wullschleger, E. *Mol. Phys.* **1975**, *29*, 305.

(56) Kaski, J.; Vaara, J.; Jokisaari, J. *J. Am. Chem. Soc.* **1996**, *118*, 8879.

(57) (a) Dewar, M. J. S. *Bull Soc. Chim. Fr.* **1951**, *18*, C71. (b) Chatt, J.; Duncanson, L. A. *J. Chem. Soc.* **1953**, 2939.

(58) Solum, M. S.; Facelli, J. C.; Michl, J.; Grant, D. M. *J. Am. Chem. Soc.* **1986**, *108*, 6464.

(59) (a) Bühl, M. *Chem. Phys. Lett.* **1997**, *267*, 251. (b) Cheeseman, J. R.; Trucks, G. W.; Keith, T. A.; Frisch, M. J. *J. Chem. Phys.* **1996**, *104*, 5497. (c) Lee, A. M.; Handy, N. C.; Colwell, S. M. *J. Chem. Phys.* **1995**, *103*, 10095. (d) Schreckenbach, G.; Ziegler, T. *J. Phys. Chem.* **1995**, *99*, 606.

(60) Jameson, A. K.; Jameson, C. J. *Chem. Phys. Lett.* **1987**, *134*, 461.